A mechanism for Rad53 to couple leading- and lagging-strand DNA synthesis under replication stress in budding yeast

Albert Serra-Cardona[a,b,c,d], Chuanhe Yu[e], Xinmin Zhang[f], Xu Hua[a,b,c,d], Yuan Yao[g], Jiaqi Zhou[g], Haiyun Gan[g,1], and Zhiguo Zhang[a,b,c,d,1]

[a]Institute for Cancer Genetics, Columbia University Irving Medical Center, New York, NY 10032; [b]Herbert Irving Comprehensive Cancer Center, Columbia University Irving Medical Center, New York, NY 10032; [c]Department of Pediatrics, Columbia University Medical Center, New York, NY 10032; [d]Department of Genetics and Development, Columbia University Medical Center, New York, NY 10032; [e]The Hormel Institute, University of Minnesota, Austin, MN 55912; [f]Department of Regenerative Medicine, School of Pharmaceutical Science, Jilin University, Changchun 130021, China; and [g]Shenzhen Key Laboratory of Synthetic Genomics, Guangdong Provincial Key Laboratory of Synthetic Genomics, Chinese Academy of Sciences Key Laboratory of Quantitative Engineering Biology, Shenzhen Institute of Synthetic Biology, Shenzhen Institutes of Advanced Technology, Chinese Academy of Sciences, Shenzhen 518055, China

Edited by Shiv I. S. Grewal, National Cancer Institute, Bethesda, MD, and approved August 9, 2021 (received for review May 20, 2021)

In response to DNA replication stress, DNA replication checkpoint kinase Mec1 phosphorylates Mrc1, which in turn activates Rad53 to prevent the generation of deleterious single-stranded DNA, a process that remains poorly understood. We previously reported that lagging-strand DNA synthesis proceeds farther than leading strand in *rad53-1* mutant cells defective in replication checkpoint under replication stress, resulting in the exposure of long stretches of the leading-strand templates. Here, we show that asymmetric DNA synthesis is also observed in *mec1-100* and *mrc1-AQ* cells defective in replication checkpoint but, surprisingly, not in *mrc1Δ* cells in which both DNA replication and checkpoint functions of Mrc1 are missing. Furthermore, depletion of either Mrc1 or its partner, Tof1, suppresses the asymmetric DNA synthesis in *rad53-1* mutant cells. Thus, the DNA replication checkpoint pathway couples leading- and lagging-strand DNA synthesis by attenuating the replication function of Mrc1-Tof1 under replication stress.

Rad53 | Mrc1 | replication stress | deleterious ssDNA | asymmetric DNA synthesis

Replication stress, broadly defined as the events that impede normal progression of DNA replication of the cell, can be induced by a variety of internal and external means (1–3). For instance, DNA lesions, deoxynucleotide triphosphate (dNTP) depletion, oncogene activation, and transcription–replication conflicts all lead to DNA replication stress (2). If left undealt with, replication stress will promote genome instability (2, 4) and drive tumorigenesis (5, 6). To meet these challenges, eukaryotic cells have developed the DNA replication checkpoint pathway to deal with various forms of replication stress, and inactivating genes in this pathway leads to genome instability in yeast and mammalian cells (3, 7–10).

At the molecular level, the checkpoint kinase Mec1 (ATR in mammals) is activated in response to DNA replication stress (3). Activated Mec1 phosphorylates the adaptor protein Mrc1 (Claspin in mammals) (11), which in turn promotes Rad53 (Chk1 in mammals) phosphorylation and activation. In the absence of Mrc1, Rad9, which in general serves as the adaptor protein for Rad53 activation in response to DNA damage, can also activate Rad53 during replication stress (12). Activated Rad53 performs multiple tasks, including 1) inhibition of late replication origin firing (13–15), 2) up-regulation of dNTP levels (16–19), and 3) prevention of replication fork collapse (20–22). Rad53 phosphorylates distinct proteins to regulate dNTP synthesis and late replication origin under replication stress. For instance, Rad53 phosphorylates Dun1, which in turn phosphorylates Sml1 and promotes Sml1 degradation (16). Sml1 is an inhibitor for ribonucleotide reductase (RNR) involved in the rate-limiting step of conversion of NTPs to dNTPs (16). Furthermore, Rad53 phosphorylates multiples sites on Sld3 and Dbf4, two proteins involved in DNA replication initiation, to inhibit late replication origin firing (14, 15, 23). Genetic studies indicate that the essential function of Mec1 (ATR) and Rad53 (Chk1) is to prevent the collapse of replication forks under replication stress (20–23), a process that lacks molecular insights. Based on the known mechanisms whereby Rad53 up-regulates dNTP levels and inhibits late replication origin firing, it is likely that Rad53 phosphorylates several proteins to prevent fork collapse under replication stress.

Recent studies indicate that Mec1 and Rad53 prevent fork collapse through inhibition of the generation of deleterious singled-stranded DNA (ssDNA) under replication stress. While short ssDNA coated by ssDNA-binding protein (RPA) is important for checkpoint activation (8, 24, 25), long stretches of ssDNAs are detected in replication checkpoint–deficient cells under replication stress in both yeast and human cells (19, 20, 26, 27). In human cells, inhibition of ATR kinase using ATR inhibitors results in excessive ssDNAs, which depletes ssDNA-binding protein RPA and leads to fork collapse and genome instability (26). Using bromodeoxyuridine (BrdU)-immunoprecipitation and strand specific sequencing (BrdU-IP-ssSeq), which can measure the relative amount of leading- and lagging-strand DNA

Significance

During the S phase of the cell cycle, the DNA replication machinery accurately duplicates the genome in spite of numerous hurdles that cause replication stress. The replication checkpoint pathway deals with the replication stress, which, if left undealt with, can lead to fork collapse and genome instability, a process that remains poorly understood. Here, we show that the DNA checkpoint pathway couples leading- and lagging-strand DNA synthesis to prevent the generation of deleterious single-stranded DNA under replication stress by attenuating the replication function of Mrc1, a protein involved in both DNA replication and replication checkpoint, providing a mechanistic insight into how eukaryotic cells overcome replication stress.

Author contributions: A.S.-C., C.Y., H.G., and Z.Z. conceived the project; C.Y. initiated the project; A.S.-C. performed experiments; X.Z. performed the Rad9 degron experiments in Fig. S1; H.G. performed analysis with help from X.H., Y.Y., and J.Z.; and A.S.-C., H.G., and Z.Z. wrote the manuscript.

The authors declare no competing interest.

This article is a PNAS Direct Submission.

See online for related content such as Commentaries.

[1]To whom correspondence may be addressed. Email: zz2401@cumc.columbia.edu or hy.gan@siat.ac.cn.

This article contains supporting information online at https://www.pnas.org/lookup/suppl/doi:10.1073/pnas.2109334118/-/DCSupplemental.

Published September 16, 2021.

synthesis in budding yeast (28), we observed that lagging-strand DNA synthesis proceeds much farther than leading strand, which leads to the exposure of long stretches of single-stranded leading-strand templates in replication checkpoint deficient *rad53-1* mutant cells under replication stress. Generation of long stretches of ssDNA at the leading-strand template is not due to nucleolytic processing of DNA by 5′-3′ Exo1 exonuclease or 3′-5′ exonuclease activity of Pol ε, Pol δ, or Mre11. Based on these results, we proposed that Rad53 couples leading- and lagging-strand DNA synthesis under replication stress. However, it is not known whether the upstream kinase Mec1 and the adaptor protein Mrc1 also function similarly to Rad53 to prevent the generation of excessive ssDNA under replication stress.

In addition to serving as an adaptor protein for Rad53 activation under replication stress, Mrc1 also functions in DNA replication under normal growth. Mrc1 is a component of the replication progression complex including Cdc45, the Mrc1-Tof1-Csm3 complex, and the histone chaperone FACT (29). Moreover, Mrc1 interacts with both Cdc45 (30) and leading-strand DNA polymerase ε (31). Mrc1 and Tof1 are recruited to DNA replication forks. In vitro, Mrc1 and Tof1-Csm3 are required for efficient DNA replication in the reconstituted DNA-replication system using purified proteins (32). Moreover, it has been shown that Mrc1 can stimulate the CMG helicase activity as well as the DNA polymerase activity (33, 34). Studies in both yeast Mrc1 and *Xenopus* Claspin indicate that the function of Mrc1/Claspin in DNA-replication checkpoint and DNA replication is separable (35, 36). For instance, deletion of Mrc1 or depletion of its mammalian homolog Claspin results in impaired S phase in a role independent of checkpoint function (35, 36). Moreover, the *mrc1-AQ* mutant containing mutations at all possible Mec1 S/TQ phosphorylation sites, while showing defects in checkpoint functions such as firing of late replication origins under replication stress, progresses through S phase normally, indicating that this mutation does not affect the replication function of Mrc1. Under replication stress, the Mrc1-Polε interaction is altered (31), and Mrc1 and Tof1 promote the formation of a stable replication-pausing complex at replication forks (30). These results suggest that the role of Mrc1 in DNA-replication checkpoint and DNA replication, while genetically separable, may be connected.

Here, we show that lagging-strand DNA synthesis also proceeds much farther than leading strands in *mec1-100* and *mrc1-AQ* mutant cells defective in DNA-replication checkpoint. Thus, coupling leading- and lagging-strand DNA synthesis under replication stress is an inherent and previously not-well-understood function of the DNA-replication checkpoint pathway. Surprisingly, the asymmetric DNA synthesis is not detected in *mrc1Δ* mutant cells in which both of the replication and checkpoint functions of Mrc1 are impaired. Furthermore, depletion of Mrc1 or Tof1 suppresses the asymmetric DNA synthesis observed in *rad53-1* mutant cells under replication stress. Thus, the replication function of Mrc1 contributes to the asymmetric DNA synthesis observed in both *rad53-1* and *mrc1-AQ* mutant cells under replication stress. Therefore, we propose that in response to DNA-replication stress, once Rad53 is activated by Mrc1, activated Rad53 will attenuate the function of Mrc1-Tof1 in DNA replication to couple leading- and lagging-strand DNA synthesis.

Results

DNA Synthesis at Lagging Strand Progresses Much Farther than Leading Strand in the *mec1-100* Mutant Cells under Replication Stress. We have shown previously that Rad53 couples leading- and lagging-strand DNA synthesis under replication stress (28). When cells with the *rad53-1* mutation, which impairs Rad53's DNA-replication checkpoint function, were treated with hydroxyurea (HU) that depletes dNTP pools and induces replication stress, lagging-strand DNA synthesis proceeds much farther than leading strand. Mec1 functions upstream of Rad53 and activates Rad53 in response to replication stress. To test whether Mec1 also functions similarly to Rad53 in regulation of DNA synthesis under replication stress, we analyzed DNA synthesis in *mec1-100* cells under replication stress using BrdU-IP-ssSeq. It is known that the *mec1-100* mutant cells are defective in the DNA-replication checkpoint but maintain the G2/M checkpoint (37, 38). Briefly, wild-type (WT) and *mec1-100* cells were arrested at G1 and then released into early S phase in the presence of HU and BrdU, a nucleotide analog incorporated into newly synthesized DNA. We then collected cells for DNA isolation and subsequent immunoprecipitation of newly synthesized DNA using antibodies against BrdU. The resulting DNA was subjected to BrdU-IP-ssSeq (Fig. 1*A*). Consistent with previous publications (28), WT cells treated with HU, while displaying no apparent effect on initiation of DNA replication from early replication origins, showed inhibition of firing of late replication origins (Fig. 1 *B–D*). Under the same conditions, late replication origins fired in both *rad53-1* (28) and *mec1-100* cells under replication stress (Fig. 1 *B–D*). Moreover, BrdU-IP-ssSeq peaks in WT cells showed a slight bias toward the leading strand (Fig. 1 *C* and *E*). In contrast, like *rad53-1* mutant cells (28), BrdU-IP-ssSeq peaks in *mec1-100* cells showed a strong lagging-strand bias at both early and late replication origins (Fig. 1 *C*, *E*, and *F*), indicating that DNA synthesis at lagging strands proceeds much farther than that of leading strands under replication stress. These results indicate that leading- and lagging-strand DNA synthesis in *mec1-100* cells are uncoupled under replication stress and that Mec1 also functions like Rad53 to regulate DNA synthesis in response to DNA replication stress.

Excessive Single-Stranded Leading-Strand Template Is Detected in *mec1-100* Mutant Cells under Replication Stress. If DNA synthesis in *mec1-100* mutant cells proceeds farther along lagging strands than leading strands, one would expect that long stretches of leading-strand template are exposed in *mec1-100* mutant cells (Fig. 2*A*). To test this idea, we analyzed the distribution of Rfa1 at replication forks in *mec1-100* cells using Rfa1 immunoprecipitation and strand-specific sequencing (ChIP-ssSeq) (39, 40). ChIP-ssSeq detects both template and newly synthesized DNA, whereas BrdU-IP-ssSeq is used to detect new synthesized DNA. Therefore, we used (+/-)bias to describe Rfa1 ChIP-ssSeq peaks, in contrast to the leading- and lagging-strand bias for BrdU-IP-ssSeq (39). Rfa1 is the large subunit of the ssDNA-binding protein RPA. Rfa1 was detected at early, but not late, replication origins in WT cells. In contrast, Rfa1 was detected in both early and late replication origins in *mec1-100* and *rad53-1* cells treated with HU (Fig. 2 *B–D*) (28), consistent with the idea that late origins fire in *mec1-100* cells. As reported previously, Rfa1 ChIP-ssSeq in WT cells showed (+) strand bias, indicating that RPA is enriched at lagging template strands in WT cells (Fig. 2 *A*, *B*, and *E*) (39). In contrast, Rfa1 ChIP-ssSeq peaks in *mec1-100* cells, like those in *rad53-1* cells (28), showed an opposite, but strong (−) bias at both early and late replication origins (Fig. 2 *B*, *E*, and *F*), indicating that RPA is enriched at leading-strand templates in *mec1-100* cells under replication stress. These results support the idea that excessive leading-strand templates compared to lagging template strand are exposed and coated with RPA in *mec1-100* cells under replication stress. Notably, these results do not exclude the possibility that single-stranded lagging-strand templates are also present in *mec1-100* cells.

Deletion of *SML1* in *mec1-100* Cells Suppresses Uncoupled DNA Synthesis at Early, but Not Late, Replication Origins. We have previously shown that deletion of *SML1*, which encodes an inhibitor for RNR, in *rad53-1* cells leads to the suppression of asymmetric DNA synthesis at early replication origins and, to a lesser extent, at late replication origins (28). We therefore analyzed the effect of *SML1* deletion in *mec1-100* cells on DNA synthesis and Rfa1 distribution at replication forks under replication stress. As shown in Fig. 3*A*, deletion of *SML1* had no apparent effects on

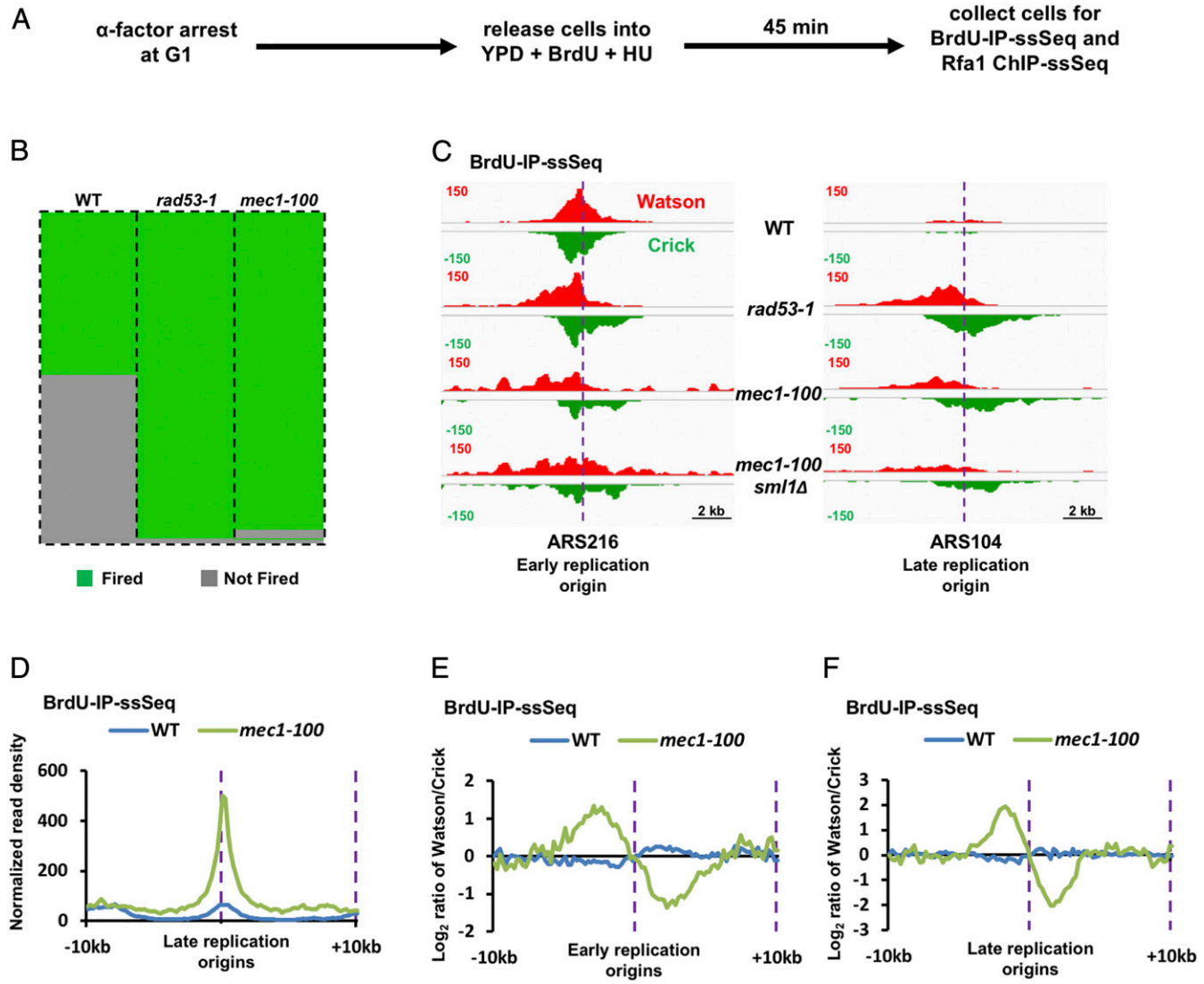

Fig. 1. The *mec1-100* mutation results in asymmetric DNA synthesis under replication stress. (*A*) Schematic representation of the experimental procedures to analyze DNA synthesis using BrdU-IP-ssSeq and to analyze the association of RPA at replication forks using ChIP-ssSeq under replication stress. (*B*) Binary representation of the firing status of DNA-replication origins in WT, *rad53-1*, or *mec1-100* cells released into S phase for 45 min in the presence of 0.2 M HU. The firing status of each DNA-replication origin is defined by the density of BrdU-IP-ssSeq. (*C*) Snapshot of BrdU-IP-ssSeq signals surrounding an early (*Left*) or late (*Right*) replication origin in cells treated with HU with their relevant genotype marked in the middle. (*D*) Normalized read density of BrdU-IP-ssSeq signals within 20 kb of late replication origins in cells treated with HU. Normalized reads per kilobase per million of mapped reads (RPKM) surrounding replication origins was calculated using a 200-bp sliding window. (*E* and *F*) The average bias of BrdU-IP-ssSeq peaks around early (*E*) or late (*F*) replication origins under HU-induced replication stress. The average $\log_2$ ratio of sequencing reads from the Watson over Crick strands of BrdU-IP-ssSeq was calculated using a 200-bp sliding window.

the firing of late replication origins in *mec1-100* cells. However, the BrdU track length in *mec1-100 sml1Δ* cells appeared to be broader than *mec1-100* cells at early replication origins, likely due to elevation of dNTP levels trigged by *SML1* deletion (Fig. 3 *B* and *C*). In contrast to the strong lagging strand bias in *mec1-100* cells, BrdU-IP-ssSeq peaks at early replication origins in *mec1-100 sml1Δ* cells showed no apparent bias. Furthermore, the strong lagging-strand bias at late replication in *mec1-100 sml1Δ* cells was also detected, albeit at a reduced amplitude compared to *mec1-100* cells (Fig. 3 *D* and *E*). These results indicate that deletion of *SML1* suppresses the asymmetric DNA synthesis at early, but not late, replication origins.

Analysis of the distribution of RPA using Rfa1 ChIP-ssSeq indicates that deletion of *SML1* in *mec1-100* cells did not affect the overall peak width at both early and late replication origins compared to *mec1-100* cells (Fig. 4 *A* and *B*). However, deletion of *SML1* in *mec1-100* cells completely suppressed the Rfa1 ChIP-ssSeq bias at early replication origins while having little effects on Rfa1 ChIP-ssSeq peak bias at late replication origins (Fig. 4 *C* and *D*). These results indicate that *SML1* deletion can suppress uncoupled DNA synthesis at early, but not late, replication origins in *mec1-100* cells under replication stress and that an increase in dNTP levels can help couple leading- and lagging-strand DNA synthesis at forks originated from early replication origins.

Uncoupled DNA Synthesis Is Detected in *mrc1-AQ*, but Not *mrc1Δ* Cells, under Replication Stress. It is known that Mec1 phosphorylates Mrc1, which in turn activates Rad53 under replication stress (3, 35). We therefore analyzed whether deletion of *MRC1* affects DNA synthesis and ssDNA generation in a manner similar

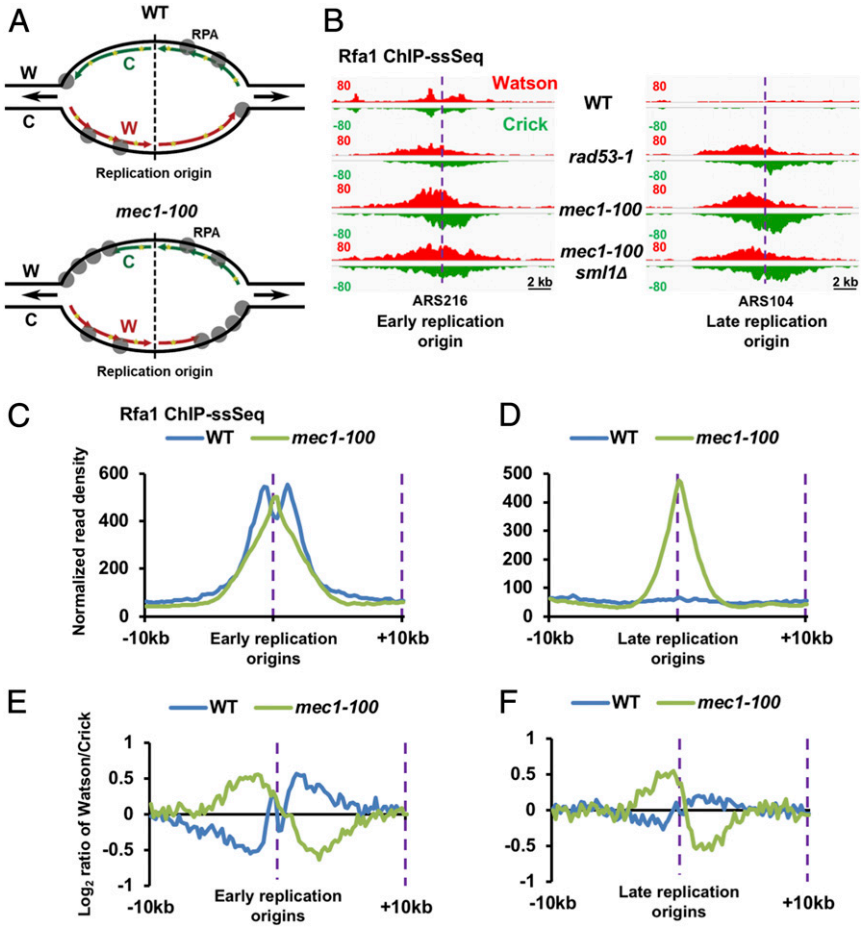

Fig. 2. Impairment of Mec1 replication checkpoint function leads to RPA accumulation on the leading-strand template under replication stress. (*A*) Schematic representation of RPA binding to single-stranded template DNA during DNA replication. RPA is enriched at lagging strands in WT cells, whereas many more RPA proteins bind to long stretches of leading template strand in *mec1-100* or *rad53-1* mutant defective in replication checkpoint. (*B*) Snapshots of Rfa1 ChIP-ssSeq signal around an early (*Left*) or late (*Right*) replication origin in cells treated with HU. (*C* and *D*) Normalized read density of Rfa1 ChIP-ssSeq signal within 20 kb of early (*C*) or late (*D*) replication origins in cells treated with HU. Reads were normalized to reads per kilobase per million of mapped reads (RPKM) and calculated using a 200-bp sliding window. (*E* and *F*) Average strand bias of Rfa1 ChIP-ssSeq peaks at early (*E*) or late (*F*) replication origins. The average $\log_2$ ratio of Rfa1 ChIP-ssSeq sequence reads from the Watson over Crick strands was calculated using a 200-bp sliding window.

to *rad53-1* and *mec1-100* mutations. Late replication origins fired in the presence of HU in *mrc1Δ* cells (Fig. 5 *A*–*C*), consistent with published studies showing that Mrc1 is important to inhibit firing of late replication origins in response to DNA-replication stress (30). The reduced BrdU density in *mrc1Δ* cells at early replication origins (Fig. 5*B*) is likely due to impaired DNA synthesis in these cells (32, 35). Surprisingly, BrdU-IP-ssSeq peaks in *mrc1Δ* cells did not show any bias toward lagging strands (Fig. 5 *D*–*E*), indicating that leading- and lagging-strand DNA synthesis is not asymmetrically affected in *mrc1Δ* cells, which is in contrast to *mec1-100* or *rad53-1* cells. Because dNTP levels in *mrc1Δ* were not elevated compared to *rad53-1* or *mec1-100* cells (41), the distinct effect of *mrc1Δ* on DNA synthesis compared to *mec1-100* and *rad53*-1 mutations is likely not due to an increase in dNTP levels in *mrc1Δ* cells.

It has been reported that Rad9 mediates Rad53 activation under replication stress in the absence of Mrc1 (12, 42). Therefore, it is possible that Rad9 functions to couple leading- and lagging-strand DNA synthesis in the absence of Mrc1. To test this idea, we made the *rad9-aid* degron in both WT and *mrc1Δ* cells and induced its degradation 30 min before cells were released from G1 phase into S phase. Rad9-auxin-inducible degron (AID) was efficiently degraded with the addition of indoleacetic acid (IAA), the plant pheromone for induction of degradation of AID-tagged proteins (*SI Appendix*, Fig. S1*A*), and Rad9 depletion had no apparent effects on the firing of late replication origins (Fig. 5*A* and *SI Appendix*, Fig. S1 *B* and *C*). BrdU-IP-ssSeq peaks from *mrc1Δ rad9-aid* cells did not show any significant bias compared to *mrc1Δ* or *rad9-aid* mutants alone (*SI Appendix*, Fig. S1 *D* and *E*), suggesting that uncoupled DNA synthesis was not detectable even in cells lacking both adaptors for Rad53 activation under replication stress.

In addition to serving as an adaptor protein for Rad53 activation during replication stress, Mrc1 also has a role in DNA replication (12, 36). The *mrc1-AQ* allele is a separation of function mutant that is defective in Mec1-mediated Rad53 activation but retains the replication function of Mrc1 (35). Therefore, we analyzed the impact of this mutant on DNA synthesis under replication stress using BrdU-IP-ssSeq. Like with *mrc1Δ* treated with HU, late replication origins also fired in *mrc1-AQ* mutant cells (Fig. 5*A*), consistent with a defect in DNA replication checkpoint in these mutant cells. In contrast to *mrc1Δ*, BrdU-IP-ssSeq peaks in *mrc1-AQ* cells showed a bias toward lagging strands (Fig. 5 *D* and *E*). This bias pattern was similar to *rad53-1* and *mec1-100* mutant cells and was opposite to that of WT and *mrc1Δ* cells. We noted that the bias amplitude of the BrdU-IP-ssSeq peaks in *mrc1-AQ* cells was smaller than that in *rad53-1* and *mec1-1* mutant

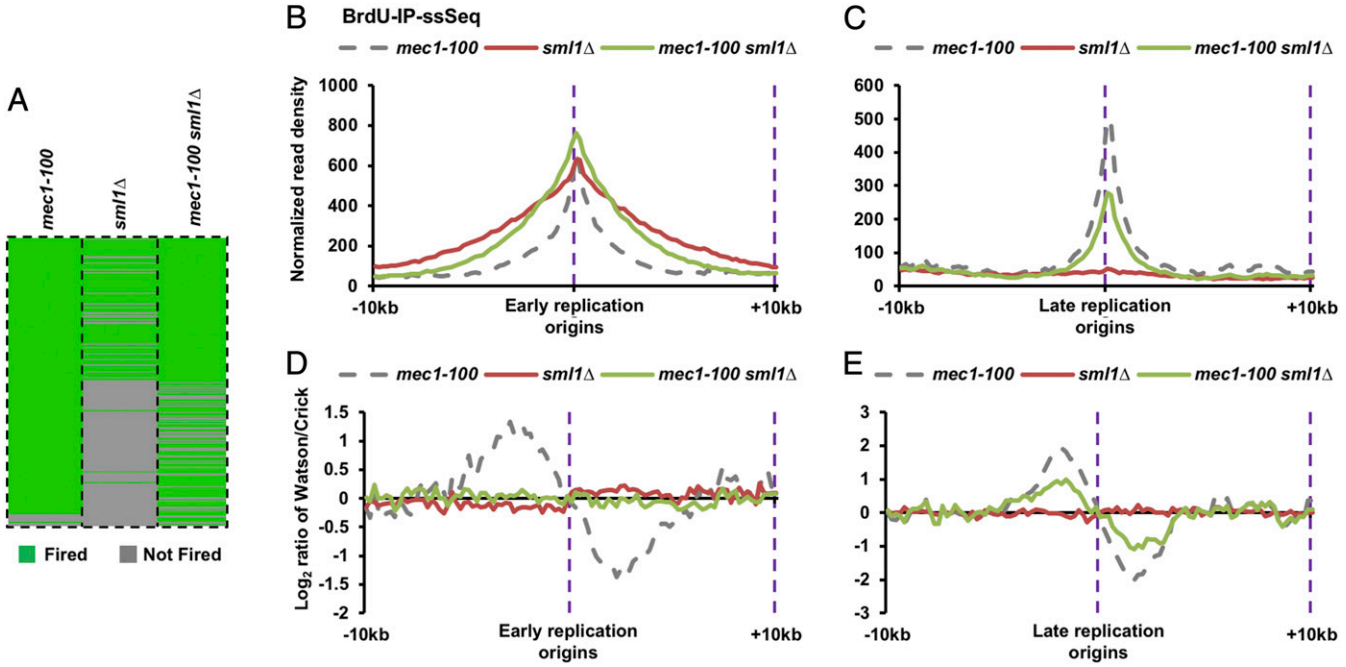

Fig. 3. Deletion of *SML1* in *mec1-100* cells suppresses the asymmetric DNA synthesis at early replication origins under replication stress. (*A*) Binary representation of the firing status of DNA-replication origins in *mec1-100*, *sml1Δ*, or *mec1-100 sml1Δ* cells treated with 0.2 M HU for 45 min. (*B* and *C*) Normalized read density of BrdU-IP-ssSeq within 20 kb of early (*B*) or late (*C*) replication origins in cells treated with HU. (*D* and *E*) The average bias of BrdU-IP-ssSeq peaks at early (*D*) or late (*E*) replication origins under replication stress by HU.

cells (compare Fig. 5 *D* and *E* to Fig. 1 *E* and *F*), suggesting that DNA synthesis at leading and lagging strands is also uncoupled in *mrc1-AQ* cells but to a lesser degree than in *rad53-1* and *mec1-100* cells.

We also asked whether depletion of Rad9 could increase the BrdU-IP-ssSeq bias in *mrc1-AQ* cells. We found that induced degradation of Rad9-AID by IAA in *mrc1-AQ* cells did not affect BrdU density at both early and late replication origins (*SI Appendix*, Fig. S2 *A*–*C*). Moreover, Rad9 depletion slightly increased the bias of BrdU-IP-ssSeq peaks at both early and late replication origins. These results suggest that Rad9 plays a minor role in coupling leading- and lagging-strand DNA synthesis in *mrc1-AQ* cells under replication stress.

Finally, we also analyzed the effect of *SML1* deletion on the asymmetric DNA synthesis in *mrc1-AQ* cells. We observed that deletion of *SML1* suppressed the asymmetric DNA synthesis at both early and late replication origins in *mrc1-AQ* cells based on

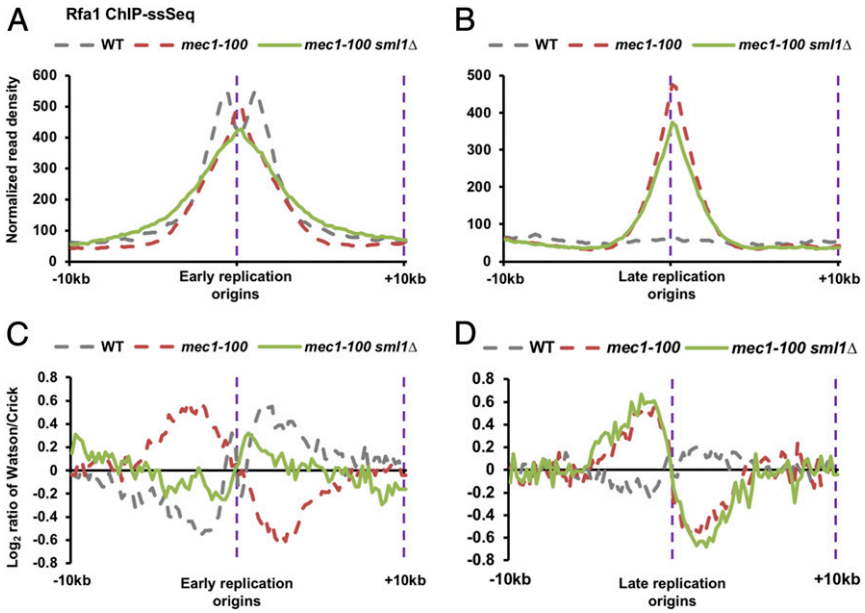

Fig. 4. Deletion of *SML1* in *mec1-100* cells suppresses the enrichment of RPA at leading-strand templates at early but not late replication origins. (*A* and *B*) Normalized read density of Rfa1 ChIP-ssSeq signal within 20 kb of early (*A*) or late (*B*) replication origins in cells treated with HU. (*C* and *D*) The average bias of Rfa1 ChIP-ssSeq at early (*C*) or late (*D*) replication origins.

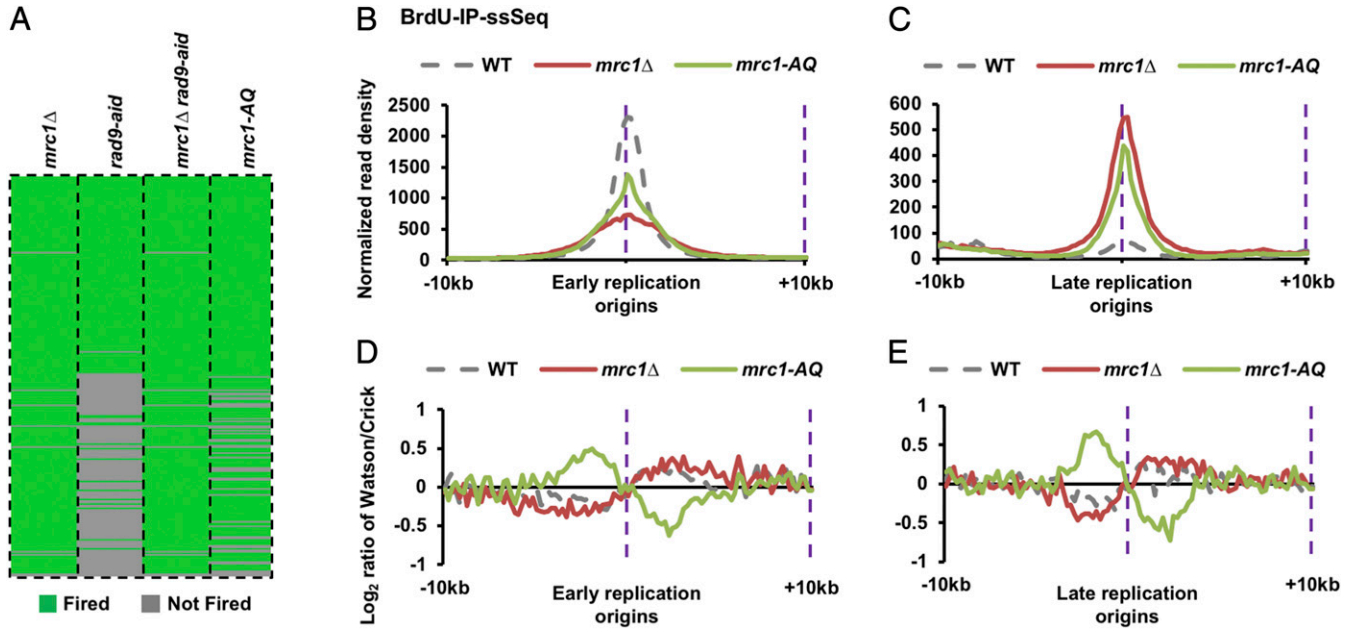

Fig. 5. The *mrc1-AQ* mutation, but not *MRC1* deletion, leads to the generation of ssDNA under replication stress. (*A*) Binary representation of early- and late-firing replication origins in *mrc1Δ*, *rad9-aid*, *mrc1Δ rad9-aid*, or *mrc1-AQ* cells treated with 0.2 M HU for 45 min. *rad9-aid* and *mrc1Δ rad9-aid* cells were treated with IAA for Rad9-AID degradation before used for BrdU-IP-ssSeq. (*B* and *C*) Normalized read density of BrdU-IP-ssSeq within 20 kb at early (*B*) or late (*C*) replication origins in cells treated with HU. (*D* and *E*) The average bias of BrdU-IP-ssSeq peaks at early (*D*) or late (*E*) replication origins in different mutant cells under HU-induced replication stress.

analysis of BrdU-IP-ssSeq bias (*SI Appendix*, Fig. S3*A* and *B*) and Rfa1 ChIP-ssSeq bias (*SI Appendix*, Fig. S3 *C* and *D*) in *mrc1-AQ sml1Δ* cells. The differential effects of *SML1* deletion on DNA synthesis at late replication origins in *mrc1-AQ* cells compared to *mec1-100* (Fig. 3*E*) and *rad53-1* cells (28) are currently unclear and warrant further investigation.

Taken together, these results indicate that while late replication origins fire in both *mrc1-AQ* and *mrc1Δ* cells under replication stress, leading- and lagging-strand DNA synthesis is uncoupled only in *mrc1-AQ* cells defective in replication checkpoint but not in *mrc1Δ* mutant cells in which both the replication and checkpoint functions of Mrc1 are impaired.

Depletion of Mrc1 or Tof1 in *rad53-1* Mutant Cells Suppresses the Asymmetric DNA Synthesis under Replication Stress. While both DNA replication and checkpoint functions are destroyed in *mrc1Δ* cells, the DNA-replication function remains intact in *mrc1-AQ* mutant cells. Therefore, we hypothesize that an intact replication function of Mrc1 contributes to the asymmetric DNA synthesis in *mrc1-AQ* cells. To explore this idea, we tested whether the replication function of Mrc1 is also needed for the observed asymmetric DNA synthesis in *rad53-1* mutant cells. We generated Mrc1-AID degron mutant in *rad53-1* mutant cells and started to deplete Mrc1 in G1 phase 30 min prior to release into S phase in the presence of HU and BrdU for analysis of DNA synthesis by BrdU-IP-ssSeq. Mrc1 was efficiently depleted with the addition of IAA (Fig. 6*A*). Moreover, depletion of Mrc1 in *rad53-1* mutant cells resulted in a slight delay in S-phase progression under normal growth conditions (*SI Appendix*, Fig. S4). Next, we analyzed how depletion of Mrc1 in *rad53-1* mutant cells affected DNA synthesis under replication stress. Depletion of Mrc1-AID in *rad53-1* cells had no apparent effect on the firing of both early and late replication origins (*SI Appendix*, Fig. S5*A*). Moreover, BrdU-ssSeq peak height was also largely unaffected upon depletion of Mrc1-AID (*SI Appendix*, Fig. S5 *B* and *C*). Remarkably, depletion of Mrc1-AID in *rad53-1* mutant cells completely suppressed the asymmetric DNA synthesis at both early and late replication origins in *rad53-1* mutant cells (Fig. 6 *B–D*). These results indicate that an intact replication function of Mrc1 also contributes to the asymmetric DNA synthesis in *rad53-1* cells under replication stress.

Mrc1 forms a complex with Tof1-Csm3 to regulate DNA replication under normal and replication stress conditions (30, 35, 43). Therefore, we tested whether deletion of Tof1 also suppresses the asymmetric DNA synthesis observed in *rad53-1* mutant cells under replication stress. Like Mrc1 depletion, Tof1 depletion in *rad53-1* mutant cells completely suppressed the asymmetric DNA synthesis at both early and late replication origins (Fig. 6 *B–D*). These results support the idea that an intact replication function of the Mrc1-Tof1 complex contributes to the asymmetric DNA synthesis and the generation of deleterious ssDNA in *rad53-1* mutant cells under replication stress. All together, these results suggest that Rad53, once activated by Mrc1 under replication stress, must attenuate the replication function of Mrc1-Tof1 to couple leading- and lagging-strand DNA synthesis under replication stress (Fig. 6*F* and *Discussion*).

rad53-1 mutant cells are highly sensitive to HU. Therefore, we tested whether Mrc1 or Tof1 depletion also suppressed HU sensitivity. Interestingly, we observed that depletion of Mrc1 or Tof1 in *rad53-1* mutant cells led to increased HU sensitivity compared to *rad53-1* mutant cells (Fig. 6*E*). These results indicate that the HU sensitivity detected in *rad53-1* mutant cells is not exclusively linked to the asymmetric DNA synthesis observed in these mutant cells treated with HU.

Mcm2 Moves ahead of DNA Synthesis in *mrc1-AQ*, but Not *mrc1Δ*, Cells Compared to WT Cells under Replication Stress. We have shown previously that both Mcm6 and Pol2 move ahead of DNA synthesis in *rad53-1* cells under replication stress (28). Others also reported that DNA-replication proteins, including Cdc45 and Pol2, move beyond DNA synthesis in *mrc1Δ* cells (30). We therefore analyzed the distribution of Mcm2, a subunit of the CMG helicase, in WT, *mrc1Δ*, and *mrc1-AQ* cells when these cells were released from G1 block into early S phase in the

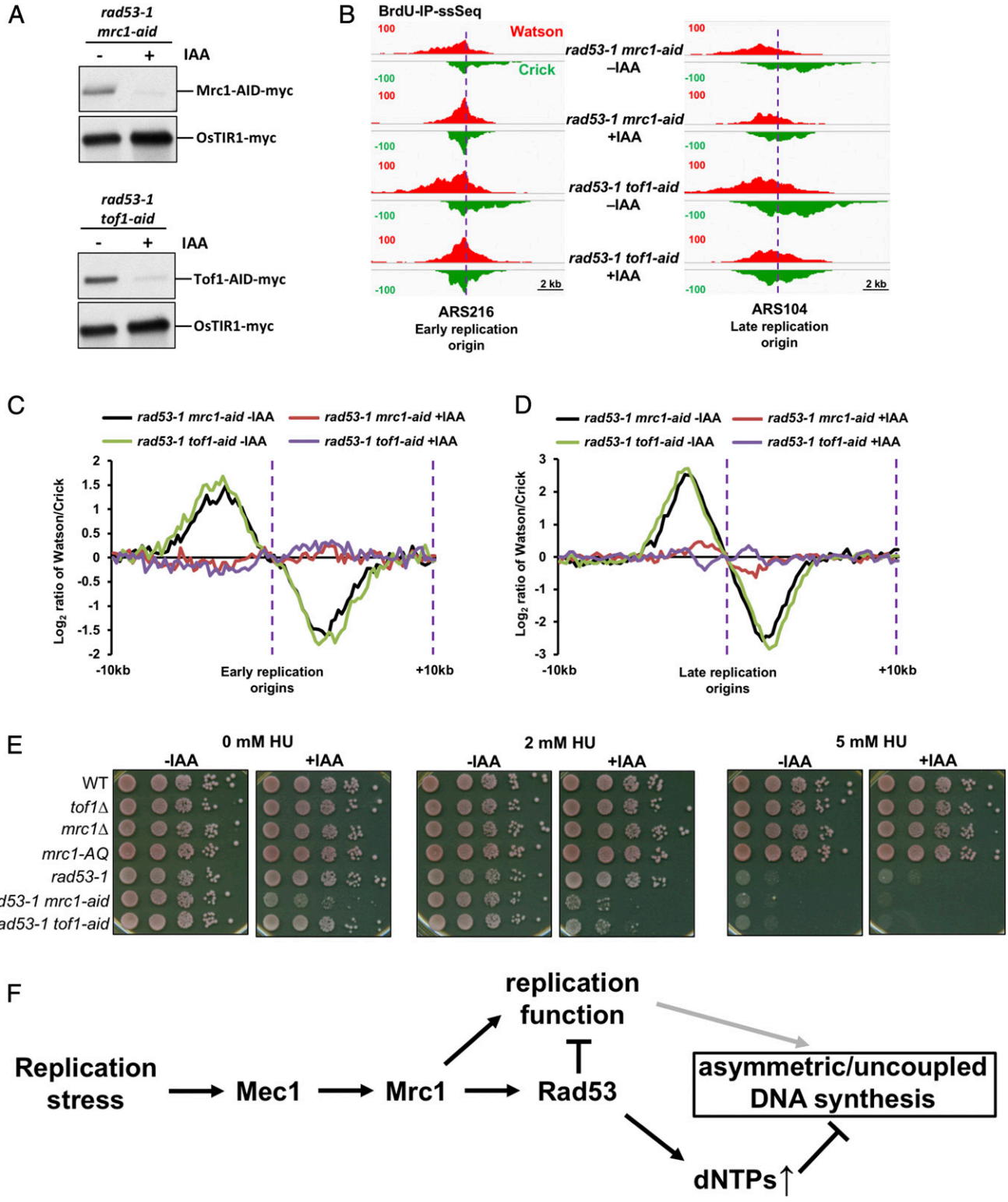

Fig. 6. Depletion of Mrc1 or Tof1 in *rad53-1* cells suppresses the asymmetric DNA synthesis under replication stress. (*A*) Western blot analysis of Mrc1-AID-myc (*Top*) or Tof1-AID-myc (*Bottom*) in the absence or presence of IAA in *rad53-1 mrc1-aid* or *rad53-1 tof1-aid* cells. IAA was added at G1 30 min before cells were released into S phase in the presence of HU and IAA. Cells were collected for BrdU-IP-ssSeq at 45 min after release. (*B*) Snapshot of BrdU-IP-ssSeq signals around an early (*Left*) or late (*Right*) replication origin in HU-treated cells with or without IAA. (*C* and *D*) Average bias of BrdU-IP-ssSeq peaks at early (*C*) or late (*D*) replication origins under replication stress by HU. (*E*) The HU sensitivity assay of the indicated strains with/without Mrc1 and Tof1 depletion by IAA. The 10-fold serial dilutions of cells were spotted on plates with/without IAA and were grown for 3 d at 30 °C before photographing. (*F*) A model for the dual role of Mrc1 to prevent deleterious ssDNA under replication stress. The gray line indicates that the replication function stimulated by Mrc1 cannot impact on the generation of deleterious ssDNA due to its inhibition by Rad53.

https://doi.org/10.1073/pnas.2109334118

presence HU and BrdU. In WT cells, we observed that Mcm2 chromatin immunoprecipitation and sequencing (ChIP-Seq) peaks displayed a valley at replication origins surrounded by two peaks, suggesting that Mcm2 travels with two forks and moves away from the site of replication initiation under this time course (*SI Appendix*, Fig. S6*A*). However, the valley of Mcm2 ChIP-Seq peaks in *mrc1Δ* and *mrc1-AQ* cells was not detectable. The functional implication of these changes in peak shape in these mutant cells compared to WT cells is not clear.

To determine whether Mcm2 moves ahead of DNA synthesis, we calculated the average peak length of Mcm2 ChIP-Seq peaks normalized against the corresponding BrdU-IP-Seq peak length in WT, *mrc1Δ*, and *mrc1-AQ* cells (*SI Appendix*, Fig. S6 *B* and *C*). We observed that the average normalized Mcm2 peak length in *mrc1Δ* was similar to that of WT cells, whereas the average Mcm2 ChIP-Seq peak length in *mrc1-AQ* cells increased compared to WT cells (*SI Appendix*, Fig. S6*C*). If we assume that Mcm2 travels the same distance as DNA synthesis (BrdU track length) in WT cells, these results indicate that Mcm2, and likely the CMG helicase, travels ahead of DNA synthesis only in *mrc1-AQ*, but not in *mrc1Δ* cells. Currently, we do not have an explanation for the discrepancy of the effect of *mrc1Δ* on the distribution of MCM proteins at replication forks described here and those reported by Katou et al. (30). One possibility is that different methods were used to analyze the distribution of replication proteins. Katou et al. utilized a ChIP-chip method based on an oligonucleotide array to analyze the distribution of replication proteins at chromosome VI with a 300-bp resolution. In contrast, we used ChIP-Seq to analyze the Mcm2 distribution genome wide at single-base-pair resolution. Nonetheless, our results are consistent with our observations that the asymmetric DNA synthesis is detected in *mrc1-AQ* but not *mrc1Δ* cells under replication stress and are also consistent with the observation that Mrc1 stimulates the helicase activity of the CMG helicase in vitro (33) (*Discussion*).

Discussion

Coupling Leading- and Lagging-Strand DNA Synthesis under Replication Stress Is an Inherent Function of the DNA-Replication Checkpoint Pathway. Previously, we reported that lagging-strand DNA synthesis proceeds much farther than leading strand synthesis in *rad53-1* cells under replication stress, resulting in the exposure of a long stretch of leading-strand template coated with RPA (28). Rad53 is an effector kinase activated by Mec1 via the adaptor protein Mrc1 in response to replication stress (3). Therefore, we tested whether mutations at *MEC1* and *MRC1* also show the same asymmetric DNA synthesis phenotypes observed in *rad53-1* mutant cells under replication stress. We found that the asymmetric DNA synthesis was also detected in *mec1-100* and *mrc1-AQ* mutant cells defective in replication checkpoint. Therefore, coupling leading- and lagging-strand DNA synthesis under replication stress is an inherent function of the DNA-replication checkpoint pathway. In vitro, leading- and lagging-strand polymerases function autonomously within a replisome (44), indicating a lack of inherent coordination between replisome components involved in leading- and lagging-strand DNA synthesis. We suggest that the lack of coordination between replisome components in the synthesis of leading and lagging strands may not affect DNA replication and cell fitness under normal growth conditions. However, under replication stress, this lack of coordination between replisome components will lead to the generation of deleterious ssDNA. Consistent with this idea, it has been shown that in the presence of a block on the leading strand, lagging-strand DNA synthesis proceeds further in *Escherichia coli* (45). We suggest that the DNA-replication checkpoint pathway in eukaryotic cells has evolved to regulate replisome components so that leading- and lagging-strand DNA synthesis is coupled under replication stress.

Mechanistically, we observed that deletion of *SML1*, which leads to an increase in dNTP concentrations, in *mec1-100*, *mrc1-AQ*, and *rad53-1* mutant cells completely suppresses the asymmetric DNA synthesis at early replication origins, while its effects on the asymmetric DNA synthesis at forks originated from late replication origins vary among checkpoint mutants analyzed with minor effects in *mec1-100* and dramatic effects in *mrc1-AQ cells*. Furthermore, depletion of Mrc1 or its partner Tof1 in DNA replication completely suppresses the asymmetric DNA synthesis in *rad53-1* mutant cells at both early and late replication origins, suggesting that the replication function of Mrc1 and Tof1, if left unchecked, contributes to the asymmetric DNA synthesis in *rad53-1* cells. Consistent with this interpretation, we detect asymmetric DNA synthesis in *mrc1-AQ* cells defective in only the checkpoint function but not in *mrc1Δ* cells in which both DNA replication and checkpoint functions are impaired. Therefore, we propose that in response to replication stress, once activated by Mec1 via adaptor protein Mrc1, Rad53 performs at least two functions to couple leading- and lagging-strand DNA synthesis: up-regulation of dNTP levels and attenuation of the replication function of Mrc1-Tof1 (Fig. 6*F* and *SI Appendix*, Fig. S7).

Why Does Deletion of *SML1* Have Differential Effects on Replication Forks Originated from Early and Late Replication Origins in *mec1-100* Mutant Cells under Replication Stress? Deletion of *SML1* in *mec1-100*, *mrc1-AQ*, and *rad53-1* mutant cells completely suppresses the asymmetric DNA synthesis of forks originated from early replication origins. In contrast, deletion of *SML1* had minor effects on the asymmetric DNA synthesis at late replication origins in *mec1-100* cells as detected both by BrdU-IP-ssSeq and RPA ChIP-ssSeq (Figs. 3 and 4). *SML1* deletion largely, but not completely, suppresses the asymmetric DNA synthesis at late replication origins in *rad53-1* cells as detected by BrdU-IP-ssSeq (28) and completely suppressed asymmetric DNA synthesis in *mrc1-AQ* cells. One likely explanation for the differential effects of *SML1* deletion on the asymmetric DNA synthesis at late replication origins in *rad53-1*, *mrc1-AQ*, and *mec1-100* cells is that these mutant alleles affect the replication checkpoint pathway to different extents. Consistent with this idea, the bias of BrdU-IP-ssSeq peaks in *mrc1-AQ* cells is the smallest. Nonetheless, these studies indicate that in both *rad53-1* and *mec1-100* mutant cells, the effect of *SML1* deletion on the asymmetric DNA synthesis at forks from early replication origins is different from that on late replication origins.

Replication at different chromosome regions in both yeast and mammalian cells occurs in a well-defined spatiotemporal program (46). In general, euchromatin regions replicate early in S phase and heterochromatin regions replicate late in S phase. In budding yeast, the majority of chromatin is euchromatic and replication origins are "site specific" and efficient. However, it is known that the chromatin environment can influence when an origin fires in the S phase of the cell cycle. For instance, when the early replication origin *ARS1* is placed near a telomere, initiation of replication from telomeric *ARS1* is delayed due to the formation of SIR-dependent heterochromatin (47). Moreover, deletion of Rpd3, a histone deacetylase, in budding yeast results in early activation of late replication origins (48). Furthermore, nucleosomes at early replication origins are different from late replication origins (49) and are a determinant factor for origin selection and functions (50). Finally, local chromatin environment can influence the loading of MCM helicase (51). Therefore, it is possible that differences in chromatin environment at early and late replication origins will impact the composition of the replisome at early and late replication origins, which in turn contributes to differential dependence of replication forks originated from early and late replication origins on dNTP levels. Future studies are needed to test this and other hypotheses.

How Does Mrc1 Couple Leading- and Lagging-Strand DNA Synthesis under Replication Stress? Mrc1 and its mammalian homolog Claspin were first discovered as the primary adaptor protein for activation of effector kinase Rad53 in yeast and Chk1 in

mammalian cells (11, 12, 36). Later on, studies from various groups indicate that Mrc1/Claspin also function in DNA replication. Moreover, the function of Mrc1/Claspin in DNA replication and DNA-replication checkpoint are separable (32, 35, 36, 52). We presented two lines of evidence supporting the idea that the DNA replication function of Mrc1 and Tof1 contributes to asymmetric DNA synthesis in checkpoint mutant cells under replication stress. First, we observed asymmetric DNA synthesis in *mrc1-AQ* mutant cells defective only in checkpoint function but not in *mrc1Δ* cells in which both replication and checkpoint functions of Mrc1 are compromised. Second, depletion of Mrc1 or Tof1 completely suppresses the asymmetric DNA synthesis in *rad53-1* mutant cells treated with HU. These results indicate that the asymmetric DNA synthesis observed in *rad53-1* mutant cells depends on the replication function of Mrc1 and Tof1. It is possible that depletion of Mrc1 or Tof1 in *rad53-1* mutant cells results in a reduced fork speed, which helps couple leading- and lagging-strand DNA synthesis under replication stress. Two observations suggest that this is unlikely the only explanation for the suppression of asymmetric DNA synthesis in *rad53-1* mutant cells. First, in the in vitro reconstituted DNA-replication reactions, Mrc1 and Tof1 stimulate DNA synthesis to different extents (32), and yet depletion of Mrc1 or Tof1 has similar/identical effects on the suppression of the asymmetric DNA synthesis in *rad53-1* mutant cells. Second, depletion of Mrc1 or Tof1 in *rad53-1* mutant cells did not affect the BrdU track length (*SI Appendix*, Fig. S5 *B* and *C*), which reflects replication-fork moving distance, to a detectable degree. Therefore, we suggest that under replication stress, the function of Mrc1 and Tof1 in DNA replication is attenuated to couple leading- and lagging-strand DNA synthesis.

Previously, it has been shown that Mrc1 interacts with several proteins involved in DNA replication. First, Mrc1 is a component of the replication progression complex (29) consisting of Cdc45, Mrc1-Tof1-Csm3, and histone chaperone FACT that is essential for chromatin replication. Cross-linking mass spectrometry analysis of Mrc1-Tof1-Csm3 in complex with the CMG helicase indicates that Mrc1 makes extensive contact with the CMG helicase (53). Second, Mrc1 also interacts with leading-strand DNA polymerase ε (31). Moreover, it has been shown that Mrc1 can stimulate the enzymatic activity of Pol ε (34). While this manuscript was under review, McClure and Diffley reported in BioRxiv that Mrc1 can stimulate the helicase activity of the CMG helicase. Furthermore, Mrc1 is phosphorylated by Rad53 (12, 35, 54), and Rad53-mediated phosphorylation of Mrc1 inactivates its ability to stimulate the helicase activity of the CMG helicase and DNA-synthesis rate (33). We have shown that Mcm2 moves ahead of DNA synthesis in *mrc1-AQ* with an intact ability to stimulate the helicase activity but not in *mrc1Δ* cells in which the ability of Mrc1 to stimulate the CMG activity is missing. Based on these results, we propose the following working model for how Mrc1 couples leading- and lagging-strand DNA synthesis under replication stress. Under normal replication conditions, Mrc1 and its partners Tof1 and Csm3 promote DNA synthesis by stimulating the activities of the CMG helicase and, possibly, Pol ε, which in turn enhance DNA synthesis. In response to replication stress, the temporary uncoupling of CMG helicase and DNA polymerases generates short ssDNA, which will be coated by RPA and serves as the platform for Mec1 activation (3, 8). Activated Mec1 phosphorylates Mrc1, which brings Rad53 closer to Mec1 for phosphorylation and activation. Activated Rad53 phosphorylates Mrc1, and this phosphorylation attenuates the ability of Mrc1 to stimulate the CMG helicase activity and thereby slows down DNA unwinding under replication stress. In this way, DNA synthesis at leading and lagging strand is coupled. Future studies are needed to test this and other models.

Materials and Methods

Yeast Strains. All yeast strains used in this study are listed in *SI Appendix*, Table S1 and were derived from W303 (*leu2-3,112 ura3-1 his3-11, trp1-1, ade2-1 can1-100*). Gene deletions were generated using a one-step replacement with marker cassettes. The *mec1-100* mutation was introduced by crossing with the strain YLL750 (38). For protein depletion, Rad9, Mrc1, or Tof1 was carboxyl-terminally tagged with AID*-9Myc using a one-step insertion into the strain YNK54 (55) with a marker cassette amplified from the plasmid pKan-AID*-9myc or pHIS-AID*-9myc (56). The BrdU-Inc (BrdU-Incorporating) vector containing the genes necessary for BrdU incorporation was introduced by crossing with strains CVy43 or CVy63 (57).

Culture Growth and Cell-Cycle Synchronization. Yeast cells grown to optical density OD_{600} = 0.4 to 0.5 in yeast extract peptone + 2% dextrose (YPD) were synchronized with α-factor (5 μg/mL, synthesized by EZBiolab) for 1.5 h at 25 °C, adding an additional 5 μg/mL α-factor after 1.5 h. G1-arrested cells were released into YPD medium at 30 °C containing 400 μg/mL BrdU (Sigma-Aldrich B5002) and 0.2 M HU (Chem-Impex 24533). A total of 45 min after release into S phase at 30 °C, cell fixation was performed with 1% paraformaldehyde for 20 min at room temperature followed by the quenching with 0.125 M glycine for 5 min at room temperature. For protein depletion experiments, IAA (Sigma-Aldrich I2886) or ethanol was added at G1, 30 min before release into S phase, at a concentration of 1 mM from a 0.5-M stock in ethanol. After cell washing at 30 °C, the same concentration of IAA was also added to medium before release.

ChIP-ssSeq and BrdU-IP-ssSeq. ChIP-ssSeq and BrdU-IP-ssSeq experiments were performed as described previously (28). Briefly, fixed cells were lysed with the glass beads beating method. Chromatin was pelleted, washed, and sheared by sonication using a Bioruptor Pico (Diagenode) to an average fragment size of 200 to 400 bp. Sheared chromatin was cleared by centrifugation followed by immunoprecipitation with anti-Rfa1 antibody (gift from Steven Brill, Rutgers University, Piscataway, NJ) or anti-Mcm2 antibody (gift from Bruce Stillman, Cold Spring Harbor Laboratory, Cold Spring Harbor, NY) and protein G Sepharose beads (GE Healthcare). DNA was recovered from both input and ChIP samples following the Chelex-100 protocol (58) and was purified with the MinElute PCR kit (QIAGEN), and strand-specific sequence libraries were prepared using the Accel-NGS 1S Plus DNA library kit (Swift BioSciences).

Input DNA obtained from the Chelex-100 extraction was used for BrdU-IP. Briefly, DNA was denatured at 95 °C for 5 min followed by incubation in an ice-water bath for 5 min. Samples were then diluted 10-fold with BrdU-IP buffer solution (1× phosphate-buffered saline), 0.0625% Triton X-100 [vol/vol], 6.7 μg/mL *E. coli* transfer ribonucleic acid, 0.40 μL/mL BrdU antibody [BD Bioscience]). After a 2-h incubation at 4 °C, 20 μL protein G Sepharose beads (GE Healthcare) was added followed by an additional 1-h incubation at 4 °C. Protein G beads were extensively washed, and DNA was eluted with 100 μL Tris-ethylenediaminetetraacetic acid buffer containing 1% sodium dodecyl sulfate (SDS) at 65 °C for 15 min. The eluted DNA was purified with Minelute PCR kit (QIAGEN) and sequenced after ssDNA library preparation using the Accel-NGS 1S Plus DNA library kit (Swift BioSciences).

Yeast Protein Extraction, SDS-PAGE (Polyacrylamide Gel Electrophoresis), and Western Blotting. Whole-cell protein extracts were prepared from 5 mL yeast culture right before fixation. Cells were collected by centrifugation, washed with cold water, and resuspended in 50 μL cold Tris-buffered saline buffer containing 1 mM dithiothreitol and 1mM phenylmethylsulfonyl fluoride. An equal amount of glass beads was added to each tube, and cells were lysed by bead beating. Lysates were transferred to new tubes, mixed with 50 μL 2× SDS-PAGE loading buffer, and boiled for 3 min. Alternatively, after washing with cold water, cells were resuspended in 300 μL 20% trichloroacetic acid and lysed by bead beating with 300 μL glass beads. Lysates were transferred to new tubes, and proteins were pelleted, resuspended in high-pH 1× SDS-PAGE loading buffer, and boiled for 4 min. For immunodetection of proteins tagged with AID*-9myc, 5 μL protein extract was resolved in an 8% SDS-PAGE, transferred onto a nitrocellulose membrane, and detected using anti-myc antibody (9E10).

HU Sensitivity Assay. Yeast strains were grown overnight at 30 °C in YPD. Cells were diluted to 6 × 10^6 cells/mL and four additional 10-fold serial dilutions and spotted onto media containing the indicated concentrations of HU and IAA (1 mM) or the same volume of ethanol. Plates were incubated at 30 °C for 3 d before pictures were taken.

Analysis of Cell-Cycle Progression. Yeast cells grown to OD_{600} = 0.4 to 0.5 in YPD were synchronized at G1 with α-factor as described in *Culture Growth and Cell-Cycle Synchronization*. To deplete Mrc1-AID or Tof1-AID, 1 mM IAA or the same volume of ethanol was added at G1 30 min before release into S phase. These cells were then collected, washed with water, and released into

YPD medium at 30 °C with or without IAA. At each indicated time point, 1 mL cell culture was harvested by centrifugation, washed with water, and fixed with 70% ethanol. Samples were further washed with 50 mM Na-citrate pH 7.4 and resuspended in the same buffer containing 250 μg/mL RNase A (Sigma-Aldrich R6513). Cells were briefly sonicated (three 1-s pulses at 30% amplitude, Sonics Vibra Cell VCX-500) and incubated at 50 °C for 1 h. Samples were then treated with 1 mg/mL Proteinase K (Invitrogen 25530015) for 1 h at 50 °C and stained with 20 μg/mL propidium iodide (Sigma-Aldrich P4170). DNA content was measured using an Attune Nxt Flow Cytometer (Thermo Fisher Scientific).

Sequence Mapping and Data Analysis. The sequence reads were mapped to the yeast genome (sacCer3) using Bowtie2 software (59). The genome-wide read coverage of Watson and Crick strands was calculated using BEDTools (60) and in-house Perl programs. To determine whether an origin fired in cells treated with HU, we used BrdU-IP-ssSeq data. Briefly, BrdU-IP-ssSeq peaks were identified by merging the sequencing reads of both Watson and Crick strands and using them for peak calling with SICER software (61) with the cutoff false discovery rate (FDR) of 0.01. If there is a detectable peak using these conditions, the origin is classified as "fired." This binary classification does not imply that an origin classified as "fired" fires in each individual cell; it means that it fired in enough cells to identify its BrdU-IP peak. Moreover, all origins used in the analysis are located at the centers of their corresponding BrdU peaks, thereby removing many origins localized at telomeres from the analysis. The majority of origins classified by this approach overlap with origins identified using other means (40). The DNA-replication origins dataset used is listed in Dataset S1. Origins were classified as "early" if there was a detectable BrdU-IP-ssSeq peak in WT cells released into S phase for 45 min in the presence of HU. Otherwise, the origin would be classified as "late." To represent the firing state of each origin in Fig. 1*B*, origins were ranked based on the cluster of the matrix of the binary value. The same ranking was used in all subsequent representations of origin firing state. To quantify the bias pattern, the $\log_2$ ratios of sequence reads of the Watson strand over the Crick strand surrounding each DNA replication origin were calculated using a 200-bp sliding window. The ratios were then normalized against the corresponding input to obtain the average bias pattern.

Quantification and Statistical Analysis. For peak calling, the FDR was calculated by SICER software (61), and the cutoff value was set to 0.01.

Data Availability. All raw and analyzed sequencing data have been deposited in the National Center for Biotechnology Information under the Gene Expression Omnibus accession number GSE172093 (62).

ACKNOWLEDGMENTS. We thank Dr. Bruce Stillman for anti-Mcm2 antibodies and Dr. Steven Brill for the antibody against yeast RPA. This work is supported by the NIH Grant R35 GM115018 (to Z.Z.), the Major Program of National Natural Science Foundation of China (Grant 32090031) and the Guangdong Provincial Key Laboratory of Synthetic Genomics (2019B030301006) (to H.G.), and the NIH Grant K99GM134180 (to A.S.-C.). The NIH/National Cancer Institute Cancer Center Support Grant P30CA013696 to the Herbert Irving Comprehensive Cancer Center supports the sequencing core facilities, which were critical for the completion of this study.

1. S. A. Hills, J. F. Diffley, DNA replication and oncogene-induced replicative stress. *Curr. Biol.* **24**, R435–R444 (2014).
2. M. K. Zeman, K. A. Cimprich, Causes and consequences of replication stress. *Nat. Cell Biol.* **16**, 2–9 (2014).
3. B. Pardo, L. Crabbé, P. Pasero, Signaling pathways of replication stress in yeast. *FEMS Yeast Res.* **17**, fow101 (2017).
4. M. Macheret, T. D. Halazonetis, DNA replication stress as a hallmark of cancer. *Annu. Rev. Pathol.* **10**, 425–448 (2015).
5. C. Tomasetti, B. Vogelstein, Cancer etiology. Variation in cancer risk among tissues can be explained by the number of stem cell divisions. *Science* **347**, 78–81 (2015).
6. C. Tomasetti, L. Li, B. Vogelstein, Stem cell divisions, somatic mutations, cancer etiology, and cancer prevention. *Science* **355**, 1330–1334 (2017).
7. A. Maréchal, L. Zou, DNA damage sensing by the ATM and ATR kinases. *Cold Spring Harb. Perspect. Biol.* **5**, a012716 (2013).
8. K. A. Cimprich, D. Cortez, ATR: An essential regulator of genome integrity. *Nat. Rev. Mol. Cell Biol.* **9**, 616–627 (2008).
9. A. Ciccia, S. J. Elledge, The DNA damage response: Making it safe to play with knives. *Mol. Cell* **40**, 179–204 (2010).
10. T. J. Berens, D. P. Toczyski, Keeping it together in times of stress: Checkpoint function at stalled replication forks. *Mol. Cell* **45**, 585–586 (2012).
11. A. Kumagai, W. G. Dunphy, Claspin, a novel protein required for the activation of Chk1 during a DNA replication checkpoint response in Xenopus egg extracts. *Mol. Cell* **6**, 839–849 (2000).
12. A. A. Alcasabas *et al*., Mrc1 transduces signals of DNA replication stress to activate Rad53. *Nat. Cell Biol.* **3**, 958–965 (2001).
13. C. Santocanale, J. F. Diffley, A Mec1- and Rad53-dependent checkpoint controls late-firing origins of DNA replication. *Nature* **395**, 615–618 (1998).
14. P. Zegerman, J. F. Diffley, Checkpoint-dependent inhibition of DNA replication initiation by Sld3 and Dbf4 phosphorylation. *Nature* **467**, 474–478 (2010).
15. J. Lopez-Mosqueda *et al*., Damage-induced phosphorylation of Sld3 is important to block late origin firing. *Nature* **467**, 479–483 (2010).
16. X. Zhao, R. Rothstein, The Dun1 checkpoint kinase phosphorylates and regulates the ribonucleotide reductase inhibitor Sml1. *Proc. Natl. Acad. Sci. U.S.A.* **99**, 3746–3751 (2002).
17. A. J. Lopez-Contreras *et al*., Increased Rrm2 gene dosage reduces fragile site breakage and prolongs survival of ATR mutant mice. *Genes Dev.* **29**, 690–695 (2015).
18. V. D'Angiolella *et al*., Cyclin F-mediated degradation of ribonucleotide reductase M2 controls genome integrity and DNA repair. *Cell* **149**, 1023–1034 (2012).
19. R. Buisson, J. L. Boisvert, C. H. Benes, L. Zou, Distinct but concerted roles of ATR, DNA-PK, and Chk1 in countering replication stress during S phase. *Mol. Cell* **59**, 1011–1024 (2015).
20. J. M. Sogo, M. Lopes, M. Foiani, Fork reversal and ssDNA accumulation at stalled replication forks owing to checkpoint defects. *Science* **297**, 599–602 (2002).
21. J. A. Tercero, M. P. Longhese, J. F. Diffley, A central role for DNA replication forks in checkpoint activation and response. *Mol. Cell* **11**, 1323–1336 (2003).
22. M. Lopes *et al*., The DNA replication checkpoint response stabilizes stalled replication forks. *Nature* **412**, 557–561 (2001).
23. B. A. Desany, A. A. Alcasabas, J. B. Bachant, S. J. Elledge, Recovery from DNA replicational stress is the essential function of the S-phase checkpoint pathway. *Genes Dev.* **12**, 2956–2970 (1998).
24. L. Zou, S. J. Elledge, Sensing DNA damage through ATRIP recognition of RPA-ssDNA complexes. *Science* **300**, 1542–1548 (2003).
25. T. S. Byun, M. Pacek, M. C. Yee, J. C. Walter, K. A. Cimprich, Functional uncoupling of MCM helicase and DNA polymerase activities activates the ATR-dependent checkpoint. *Genes Dev.* **19**, 1040–1052 (2005).
26. L. I. Toledo *et al*., ATR prohibits replication catastrophe by preventing global exhaustion of RPA. *Cell* **155**, 1088–1103 (2013).
27. G. Pellicanò *et al*., Checkpoint-mediated DNA polymerase ε exonuclease activity curbing counteracts resection-driven fork collapse. *Mol. Cell* **81**, 2778–2792.e4 (2021).
28. H. Gan *et al*., Checkpoint kinase Rad53 couples leading- and lagging-strand DNA synthesis under replication stress. *Mol. Cell* **68**, 446–455.e3 (2017).
29. A. Gambus *et al*., GINS maintains association of Cdc45 with MCM in replisome progression complexes at eukaryotic DNA replication forks. *Nat. Cell Biol.* **8**, 358–366 (2006).
30. Y. Katou *et al*., S-phase checkpoint proteins Tof1 and Mrc1 form a stable replication-pausing complex. *Nature* **424**, 1078–1083 (2003).
31. H. Lou *et al*., Mrc1 and DNA polymerase epsilon function together in linking DNA replication and the S phase checkpoint. *Mol. Cell* **32**, 106–117 (2008).
32. J. T. P. Yeeles, A. Janska, A. Early, J. F. X. Diffley, How the eukaryotic replisome achieves rapid and efficient DNA replication. *Mol. Cell* **65**, 105–116 (2017).
33. A. W. McClure, J. F. Diffley, Rad53 checkpoint kinase regulation of DNA replication fork rate via Mrc1 phosphorylation. *Elife* **10**, 10.7554/eLife.69726 (2021).
34. Z. X. Zhang, J. Zhang, Q. Cao, J. L. Campbell, H. Lou, The DNA Pol ε stimulatory activity of Mrc1 is modulated by phosphorylation. *Cell Cycle* **17**, 64–72 (2018).
35. A. J. Osborn, S. J. Elledge, Mrc1 is a replication fork component whose phosphorylation in response to DNA replication stress activates Rad53. *Genes Dev.* **17**, 1755–1767 (2003).
36. J. Lee, A. Kumagai, W. G. Dunphy, Claspin, a Chk1-regulatory protein, monitors DNA replication on chromatin independently of RPA, ATR, and Rad17. *Mol. Cell* **11**, 329–340 (2003).
37. J. A. Cobb *et al*., Replisome instability, fork collapse, and gross chromosomal rearrangements arise synergistically from Mec1 kinase and RecQ helicase mutations. *Genes Dev.* **19**, 3055–3069 (2005).
38. V. Paciotti, M. Clerici, M. Scotti, G. Lucchini, M. P. Longhese, Characterization of mec1 kinase-deficient mutants and of new hypomorphic mec1 alleles impairing subsets of the DNA damage response pathway. *Mol. Cell. Biol.* **21**, 3913–3925 (2001).
39. C. Yu, H. Gan, Z. Zhang, Both DNA polymerases δ and ε contact active and stalled replication forks differently. *Mol. Cell. Biol.* **37**, e00190-17 (2017).
40. C. Yu *et al*., Strand-specific analysis shows protein binding at replication forks and PCNA unloading from lagging strands when forks stall. *Mol. Cell* **56**, 551–563 (2014).
41. J. Poli *et al*., dNTP pools determine fork progression and origin usage under replication stress. *EMBO J.* **31**, 883–894 (2012).
42. J. Bacal *et al*., Mrc1 and Rad9 cooperate to regulate initiation and elongation of DNA replication in response to DNA damage. *EMBO J.* **37**, e99319 (2018).
43. M. Bando *et al*., Csm3, Tof1, and Mrc1 form a heterotrimeric mediator complex that associates with DNA replication forks. *J. Biol. Chem.* **284**, 34355–34365 (2009).
44. J. E. Graham, K. J. Marians, S. C. Kowalczykowski, Independent and stochastic action of DNA polymerases in the replisome. *Cell* **169**, 1201–1213.e17 (2017).
45. V. Pagès, R. P. Fuchs, Uncoupling of leading- and lagging-strand DNA replication during lesion bypass in vivo. *Science* **300**, 1300–1303 (2003).
46. N. Rhind, D. M. Gilbert, DNA replication timing. *Cold Spring Harb. Perspect. Biol.* **5**, a010132 (2013).
47. J. B. Stevenson, D. E. Gottschling, Telomeric chromatin modulates replication timing near chromosome ends. *Genes Dev.* **13**, 146–151 (1999).

48. J. G. Aparicio, C. J. Viggiani, D. G. Gibson, O. M. Aparicio, The Rpd3-Sin3 histone deacetylase regulates replication timing and enables intra-S origin control in *Saccharomyces cerevisiae*. *Mol. Cell. Biol.* **24**, 4769–4780 (2004).
49. I. Soriano, E. C. Morafraile, E. Vázquez, F. Antequera, M. Segurado, Different nucleosomal architectures at early and late replicating origins in *Saccharomyces cerevisiae*. *BMC Genomics* **15**, 791 (2014).
50. M. L. Eaton, K. Galani, S. Kang, S. P. Bell, D. M. MacAlpine, Conserved nucleosome positioning defines replication origins. *Genes Dev.* **24**, 748–753 (2010).
51. J. A. Belsky, H. K. MacAlpine, Y. Lubelsky, A. J. Hartemink, D. M. MacAlpine, Genome-wide chromatin footprinting reveals changes in replication origin architecture induced by pre-RC assembly. *Genes Dev.* **29**, 212–224 (2015).
52. S. J. Szyjka, C. J. Viggiani, O. M. Aparicio, Mrc1 is required for normal progression of replication forks throughout chromatin in *S. cerevisiae*. *Mol. Cell* **19**, 691–697 (2005).
53. D. Baretić *et al*., Cryo-EM structure of the fork protection complex bound to CMG at a replication fork. *Mol. Cell* **78**, 926–940.e13 (2020).
54. M. C. Lanz *et al*., In-depth and 3-dimensional exploration of the budding yeast phosphoproteome. *EMBO reports* **22**, e51121 (2021).
55. K. Nishimura, T. Fukagawa, H. Takisawa, T. Kakimoto, M. Kanemaki, An auxin-based degron system for the rapid depletion of proteins in nonplant cells. *Nat. Methods* **6**, 917–922 (2009).
56. M. Morawska, H. D. Ulrich, An expanded tool kit for the auxin-inducible degron system in budding yeast. *Yeast* **30**, 341–351 (2013).
57. C. J. Viggiani, O. M. Aparicio, New vectors for simplified construction of BrdU-Incorporating strains of *Saccharomyces cerevisiae*. *Yeast* **23**, 1045–1051 (2006).
58. J. D. Nelson, O. Denisenko, K. Bomsztyk, Protocol for the fast chromatin immunoprecipitation (ChIP) method. *Nat. Protoc.* **1**, 179–185 (2006).
59. B. Langmead, S. L. Salzberg, Fast gapped-read alignment with Bowtie 2. *Nat. Methods* **9**, 357–359 (2012).
60. A. R. Quinlan, I. M. Hall, BEDTools: A flexible suite of utilities for comparing genomic features. *Bioinformatics* **26**, 841–842 (2010).
61. C. Zang *et al*., A clustering approach for identification of enriched domains from histone modification ChIP-Seq data. *Bioinformatics* **25**, 1952–1958 (2009).
62. A. Serra-Cardona *et al*., Next-generation sequencing datasets. National Center for Biotechnology Information *Gene Expression Omnibus* (NCBI GEO). https://www.ncbi.nlm.nih.gov/geo/query/acc.cgi?acc=GSE172093. Deposited 14 August 2021.